Role of Exosomes in B cell development and antibodies class switching recombination

Submitted by Ho Wai Yim as a thesis for the degree of Master by Research in Biological Science in February 2019

I certify that all material in this thesis which is not my own work has been identified and that no material has previously been submitted and approved for the award of a degree by this or any other University.

Signature: ……..

1 Acknowledgement

I would like to thank Dr. Richard Chahwan who provided the projects. Thank you for the opportunity and for the support throughout.

I would also like to thank Rikke Morrish, Laurence Higgins, Laura Reffo, Emily Sheppard and Sally Rogers for creating a pleasing work experiment

2 Abstract

Exosomes are nanoparticles being released by various types of cells and they often carry functional cargo, including RNA and proteins, and provide a means to shuttle these cargos between cells. Emerging evidence suggest that exosomes are vital player in process such as intercellular communication and indirect gene regulation through protein and non-coding RNA cargo. The ability of efficient and secure exosome-mediated molecules transfers leads to a novel avenue to understand immune response regulation towards diseases and cancers. Several research groups have proven that exosomes are involved in intercellular communication between dendritic cells, T cells and B cells. Nonetheless, B-to-B cell communication and regulation of adaptive immune response via exosomal pathway haven't been well studied. In this thesis, we investigated the role of exosomes in B cell development and antibody class switching recombination (CSR), an important process in adaptive immune response where mature B cells respond to antigens and secret classes of antibodies in order to diversify antibodies' effector function. We observed CSR impairment under the depletion of bovine exosomes in cell medium and endogenous exosomes derived from CH12, a murine B lymphoma cell line.. Interestingly, complement of exosomes from naïve CH12 appear to be suppressive for CSR whilst exosomes from activated CH12 show a facilitating effect. Preliminary investigation in exosomal RNA showed selective packaging of exosomal cargo during CSR and such findings could provide a more accurate direction in understanding exosome-mediated regulation in CSR.

Table of Contents

3 List of Figures

4 Introduction

Exosomes are cell-derived lipid nanoparticles that can be found in numerous biofluid sources, including blood, urine, tears, and breast milk. Exosomal particle dimensions range from 30 to 100 nm in diameter (1). The biogenesis of exosomes is widely believed to involve multiple cellular stages, inward budding of endosomal membrane that forms the multivesicular bodies (MVBs), transfer of MVBs to the plasma membrane, merge of MVBs with the plasma membrane and release of internal vesicles to the extracellular space (2). A vast majority of cell types, including cells grown in culture, generate and release exosomes, and emerging findings is showing that exosomes participate in number of biological processes including intercellular communication and antigen presentation in diverse aspects such as immune modulation and cancer proliferation (3). Studies have shown that most of the content of exosomes reflect their parental cell of origin. This useful feature allows exosomes to serve as the next generation biomarker for clinical diagnosis and therapy (4). Such intercellular communication is mainly facilitated by the active packaging of cargos, including DNA, RNA, proteins and lipids in a selective manner. The shuttling of the mixed cargos between cell of origin and targeted recipient cells is surprisingly efficient and reliable due to the apparent stability of exosomes in body fluids (5). For example, in vitro studies have shown that exosomal miRNA is able to downregulate known target genes in distant recipient cells (6). However, little is known about the network of biological processes exosomes involved and there are still many technical limitations which make them even more challenging to study.

Detection and quantification of exosomes are still not very well established due to their small sizes and the technical difficulties associated with detecting them using either flow cytometry or conventional light microscopy. That is why, Transmission

electron microscopy (TEM) is currently still the golden standard of exosome detection but the whole process requires extensive sample preparation (7). Nanoparticle tracking analysis (NTA) has been widely used for detection and quantification of exosomes due to its shorter sample preparation time compared to TEM. Briefly, NTA measure the concentration and sizes of particles by relating the rate of Brownian motion to particle size but the accuracy of this approach can be affected by the instrument settings and calibration (8). Flow cytometry has been emerging as a robust and fast way to detect and quantify exosomes. Moreover, flow cytometry allows multiplex fluorescence detection which means molecular information is available alongside. These properties are especially useful for clinical applications such as diagnosis and prognosis (9). However, a dedicated set up is essential to provide accurate sizing of nanoparticles as the detection limit of conventional flow cytometers are around 500 nm. Also, dedicated set up requires a considerably powerful flow cytometer and lengthy process of trial and error for detection of exosomes coming from different cell origins. Here, we attempted to develop a flow cytometry-based method using B cell-specific antibody coated beads that are readily and accurately detectable by conventional flow cytometer. Using this method, we expected to quantify exosomes shredding from inactivated and activated B cells.

It has been reported that CD8 T cell-mediated immune response is triggered and modulated by B cell-derived exosomes (10). Interestingly, recent studies have shown that B lymphoma cells utilize exosomal pathway(s) to evade humoral immunotherapy by releasing exosomes that carry their own surface antigen (Ag) CD20, binding to a highly utlilized therapeutic anti-CD20 antibodies called Rituximab, thereby neutralizing complement and shielding the cancer cells from antibody-based immune-therapy (11). This indicates the exosome is a courier platform shared

between normal and cancer immune cells for diverse vital purposes.

Another unexpected aspect of exosomes is that it has a rather different profile of content compared to that of their parental cells, especially RNA. Generally, exosomal cargo mirrors the abundance and types of the parental cellular content based on the biogenesis of exosomes which involves inward budding of the endosomal membrane. However, several studies have discovered that specific RNAs are enriched in exosomes as compared to parental cells. For instance, a subset of miRNA with potential role in endocytosis regulation are enriched in 293T derived exosomes; MiR-451 is found persistently enriched in exosomes in many cell types such as breast cancer cells lines and mesenchymal stem cells (12). Such discrepancy in RNA abundance and types between exosomes and parental cells suggesting the packaging of exosomal cargo isn't a passive process and the underlying selective loading mechanisms are under intensive investigation.

In this study, we investigated the role of exosomes in B cell intercellular communication including B cell development and immunoglobulin class switching recombination (CSR). CSR is a unique process in adaptive immune response that allow B cells to produce different classes of antibodies after activation by T cell cytokines. During CSR, double-stranded breaks occur at the switch (S) regions of the antibody heavy chain locus at 2 selected sites facilitated by series of enzymes including Activation-Induced (Cytidine) Deaminase (AID). The DNA locus between the 2 selected sites on S regions are removed from the chromosome, namely μ and δ constant gene segments which encode for immunoglobulin (Ig) M and IgD respectively in inactivated naïve B cells. The removal of the selected S regions is followed by substitution of γ, α, ε constant genes which encode for IgG, IgA and IgE respectively. The 2 free DNA ends of S regions are then rejoined by non-homologous

end joining (NHEJ) and resulting in the expression of switched antibody class (13).

The current understanding of CSR regulation is mainly based on antigen recognition, T cell binding, and cytokine induction which together culminate in the maturation of B cells and stimulation of AID mutagenic activity (13). Interestingly, miR-155, a common exosomal RNA cargo across many cell types, was shown to directly downregulate AID expression which can possibly lead to downregulation of CSR in B cells (14). This leaded to a new path for us to discover the possibility of CSR modulation at the post-transcriptional level via exosomal pathway, especially exosomal RNA. In this study, we use CH12, a murine B lymphoma cell line as a study model since they switch predominantly μ to α percentage (up to 50%) which gives robust and reliable result compared to primary B cells which able to switch to either IgG1 or IgG3 up to 30% and 10% respectively. Therefore, CH12 serves a better model in this study During CSR, around 30% of the CH12 population was activated and switched from IgM to IgA with IL-4/TGF-β/CD40-L stimulation and such isotype switching act as a checkpoint in B cell development. We identified exosome-facilitated intercellular communication is an alternative pathway to regulate CSR. B cell endogenous exosomes formation was reduced with GW4869, inhibitor of neutral-sphingomylelinase (n-SMase) which has been shown to inhibit exosome release from cells (15). We found decreased endogenous exosome production lead to a significant reduction of CSR efficiency. Surprisingly, the depletion of exogenous exosomes in culture medium also lead to significant reduction of CSR efficiency up to 50%. This indicated that both endogenous and exogenous exosomes might share common molecular packages that are responsible for CSR modulation. To validate the responsible role of exosomes in CSR modulation, we attempted to activate GW4869-treated CH12 to undergo CSR with the supplement of exosomes derived from bovine serum, inactivated CH12 and activated CH12 separately.

Interestingly, reduction of CSR efficiency caused by depletion of endogenous and exogenous exosomes, can be reconstituted by the addition of both bovine serum and activated CH12-derived exosomes but not the inactivated CH12-derived exosomes.

It has been reported that the molecular components in exosomes are mostly small RNA and there are evidence showing that exosomal miRNA take part in intercellular gene expression regulation in a targeted manner (16). Furthermore, there are evidences showing both exogenous- and endogenous-derived non-coding RNAs can indirectly modulate CSR by mediating precise AID targeting (17). Another well-known characteristics of non-coding RNAs (ncRNA) is the ability to control gene expression at the post-transcriptional level via sequence specific interaction with the regulatory sites. In the context of exosomal cargo shuttling, exosomal ncRNAs not only affecting their host cells' gene expression, they can also manipulate gene expression in neighbour cells as well as distant cells, possibly across different cell types or between lesion cells and normal cells. To understand whether B cells also exploit such a pathway to regulate CSR, i) we investigated the role that small and longncRNA play in both CH12 cells and their corresponding exosomal cargo. From this set of paired cell and exosomes samples, ii) we quantified expression differences in multiple RNA classes as well as essential genes required for CSR, namely AID (gene that encode activation-induced (cytidine) deaminases that initiate CSR via causing mismatch on Switch region), Sα (encoding for IgA), Sμ (encoding for IgM) and Sμ-lariat (intronic RNA lariat required for targeting of AID to Switch region via debranching of lariat) between cells and exosomes, pre- and post-activation for CSR, to identify significant differentially expressed transcripts in cells versus exosomes and iii) to elucidate the underlying gene regulation network of CSR in the exosomal pathway.

5 Materials and methods

5.1 Cell culture

CH12 cells were grown at 37 °C and 5% CO_2 in RPMI 1640 (GE Healthcare Hyclone) supplemented with 10% heat-inactivated fetal calf serum (Gibco, Life Technologies), 50 U/mL penicillin/streptomycin (Gibco, Life Technologies), 5% NCTC-109 medium (Gibco, Life Technologies), 2 mM L-glutamine (Gibco, Life Technologies), 1 mM sodium pyruvate (Gibco, Life Technologies), 50 μM 2-mercaptoethanol (Gibco, Life Technologies). Primary B cells were grown at 37 °C and 5% CO_2 in RPMI 1640 (GE Healthcare Hyclone) supplemented with 10% heat-inactivated fetal calf serum (Gibco, Life Technologies), 50 U/mL penicillin/streptomycin (Gibco, Life Technologies), 2 mM L-glutamine (Gibco, Life Technologies), 1 mM sodium pyruvate (Gibco, Life Technologies), 50 μM 2-mercaptoethanol (Gibco, Life Technologies)

5.2 Endogenous exosome inhibition and CH12 CSR

CH12 cells were pre-treated with GW4869 (10 mM Sigma Aldrich) for 2 hours and washed with 1 × PBS twice. Washed cells were grown in bovine exosome-depleted media supplemented with GW4869 and stimulated to undergo CSR. Bovine exosomes were depleted by overnight centrifugation at 120,000 × g. In short, CH12 cells were stimulated with 20 ng/mL IL-4, 1 μg/mL monoclonal anti-CD40 and 1 ng/mL TGF-β at 2 × 10^5 cells/mL and cells were collected 48 hours for downstream assays and exosome isolation. Splenic primary B cells were isolated from wild type C57BL/6 female mice (>6 weeks old) and stimulated to undergo CSR with 20 ng/ml IL-4, 2 μL/culture medium lipopolysaccharide (LPS) solution (500X) (eBioscience) at 2 × 10^5 cells/mL and cells were collected every 24 hours for downstream assays and exosome isolation

5.3 Exosome isolation

48 hours after cytokine stimulation, CH12 cells at 1 × 10^6 cells/mL were washed with sterile PBS twice and allowed to grow in bovine exosome-depleted media for 24 hours reaching maximum density of 2 × 10^6 cells/mL. Bovine exosomes were depleted by overnight centrifugation at 120,000 × g. To collect CH12 exosomes, CH12 cells were pelleted at 300 × g for 5 minutes and saved for RNA collection and surface Ig detection by flow cytometry. The remaining medium was centrifuged at 10,000 × g for 15 minutes and then subjected to ultracentrifugation at 110,00 × g for 70 minutes to pellet exosomes (Type 42.1 rotor). Exosomes pellet were washed in 1 × PBS and centrifuged again at 110,000 × g for 70 minutes (Type 42.1 rotor). All centrifugation was performed in 4 °C.

5.4 Exosome characterization

Exosomes isolated from CH12 were characterized by transmission electron microscopy and flow cytometry (BD Accuri C6 plus). For flow cytometry, 'homemade' antibody coated beads were used according to (17). Briefly, 3 μm latex beads (Sigma Aldrich) were incubated with anti-CD63 (Santa Cruz Biotechnology) overnight at room temperature. Purified CH12 exosomes were then incubated with the antibody coated beads overnight at 4 °C. Exosome-bead complexes were washed with wash buffer then incubated with FITC-anti-IgM (BD Pharmingen) in dark for 40 minutes at 4 °C before data acquisition.

5.5 Flow cytometry analysis of CH12

CH12 cells were pelleted and washed in 1 × PBS twice and incubated with APC-anti-IgM (1:200 BD Pharmingen) and FITC-anti-IgA (1:200 BD Pharmingen) in dark for 40 minutes at 4 °C before data acquisition using flow cytometer (BD Accuri C6 plus).

Primary B cells were washed in 1 × PBS twice and incubated with APC-anti-IgG1 (1:200 ebioscience) and FITC-anti-IgM (1:200 BD Pharmingen) in dark for 40 minutes at 4 °C before data acquisition using flow cytometer (BD Accuri C6 plus).

5.6 RNA extraction using TRI reagent and tapestation analysis

1 mL of TRI reagent (Invitrogen) were used to lyse CH12 cell pellet and exosome pellet. 200 µL of chloroform was added to the homogenized mixture and centrifuged at 12,000 × g for 15 minutes at 4 °C. RNA in the aqueous phase was precipitated by adding 500 µL of isopropanol and centrifuged at 12,000 × g for 10 minutes at 4 °C. RNA pellet was washed with 75% ethanol and centrifuged at 7,500 × g for 5 minutes at 4 °C. RNA pellet was left to air dry briefly and dissolved in nuclease-free water. RNA quality and quantity were examined using an Agilent 2200 Tapestation bioanalyzer (Agilent Technologies, Santa Clara, CA). 5 µL of RNA sample buffer was mixed with 1 µL RNA sample. The sample mixture was heated at 72 °C for 3 minutes then placed on ice for 2 minutes. RNA samples were loaded to the 2200 Tapestation instrument for data acquisition. RNA quality and quantity were analyzed in the 2200 Tapestation controller software, electropherogram and gel electrophoresis images were generated in the software.

5.7 Real time quantitative polymerase chain reaction

Eluted exosomal RNA were reverse transcribed to cDNA (ProtoScript® II First Strand cDNA Synthesis Kit) and qPCR was performed in triplicates using Brilliant II SYBR green (Agilent) and Rotor-Gene Q (Qiagen), transcripts quantities were normalized to β-actin.

Primers: murine AID (F) CTCCTGCTCACTGGACTTCG, murine AID (R) AGGCTGAGGTTAGGGTTCCA. murine B-Actin(F) GGCTCCTAGCACCATGAAG, murine B-Actin(R)GAAAGGGTGTAAAACGCAGC, SµGLT(F)

CTCTGGCCCTGCTTATTGTTG, SμGLT(R) AATGGTGCTGGGCAGGAAGT,

SαGLT(F) CCAGGCATGGTTGAGATAGAGATAG, SαGLT(R)

GAGCTGGTGGGAGTGTCAGTG, Sμ lariat(F)

AAGAGTAGCAACAAGGAAATAGCAG, Sμ lariat(R)

GCAGAAACAGTTTACAAGCTTTAAGA (18)

6 Results

6.1.1 Characterization of exosomes derived from CH12 by TEM

Exosomes derived from CH12 were isolated by serial ultracentrifugation method (Fig 1A). To validate the method, we investigated the sizes and the morphology of the purified exosomes. Transmission electron microscopy (TEM) was used to image exosome from pellets or from serum suspensions. The content was fairly homogenous particles with bilayer membrane of sizes around 50 nm in diameter (Figure 1B). The cup-shaped morphology and the average size of the purified CH12 exosomes confirmed the typical feature of exosomal particles and exosomes derived from other types of B cells (19).

6.1.2 Characterization of exosomes derived from CH12 by immuno-gold TEM after CSR

Exosomes were shown to incorporated with antigens from their parental antigen-presenting cells and able to modulate immune responses between dendritic cells and T cells through such characteristics (10) (20). In order to understand whether surface immunoglobulin (Ig) on B cells is being shuttled into the exosome pathway, we applied immunogold labelling to detect the presence of B cell specific Igs on primary- and CH12- derived exosomes on B cell surface. We successfully detected IgM on the surface of purified exosomes derived from inactivated CH12 (Fig. 1C) which agreed with previous characterization of B cell exosomes (19). Around 30% of the CH12 population's surface Ig switches from IgM to IgA 48 hours during CSR. We tried to understand whether the amount of exosomal surface Ig released from switched cells could reflect their parental surface isotype. We applied immunogold labelling approach to characterize exosomes derived from inactivated and activated CH12. IgM were detected on the surface of both inactivated and activated CH12

exosomes, however, the density difference of IgM is not noticeable (Fig 1D).

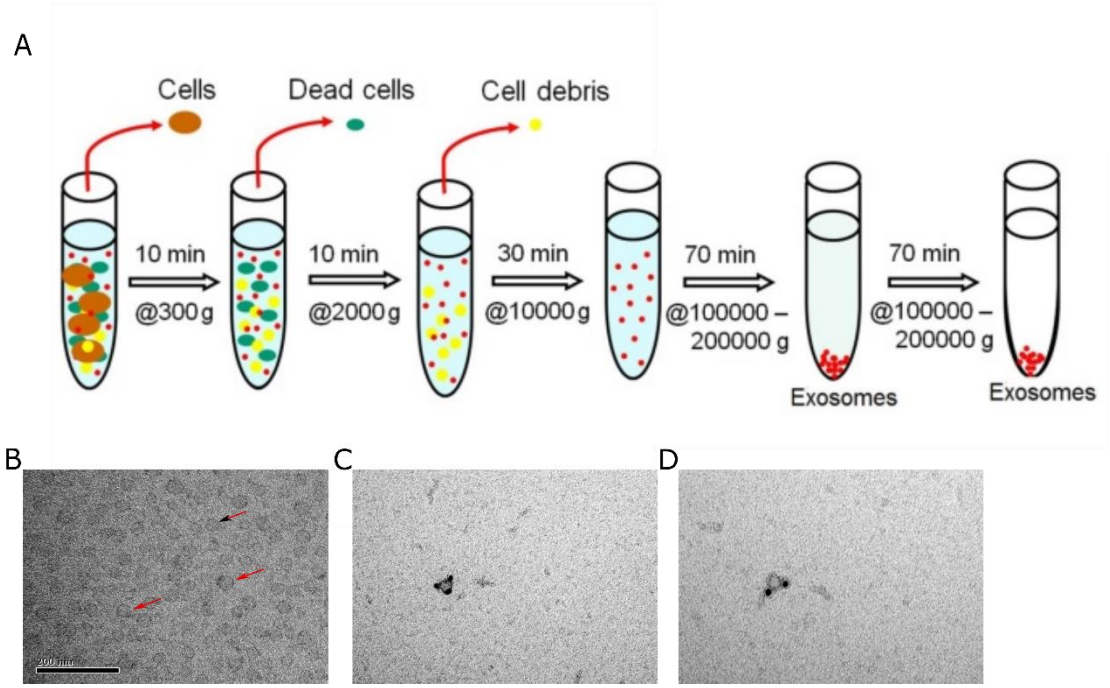

Fig.1 *Detection and Quantification of EV isolated from supernatants of CH12, a murine B lymphoma cell line*. A) Schematic outline of exosome purification by serial ultracentrifugation. B) TEM of isolated CH12 exosomes. Red arrows indicate isolated examples. Bar, 200 nm. C) Immuno-gold labelling (anti-IgM) of exosomes from unswitched CH12. Black dots indicate presence of IgM. D) Immuno-gold labelling (anti-IgM) of exosomes from activated CH12. Black dots indicate presence of IgM.

6.1.3 Characterization of exosomes in primary B cells and CH12 by FACS

Aside from TEM and immunogold labelling, flow cytometry is also adopted to characterize exosomes due to its ability for easy and fast high-throughput qualitative and quantitative analysis as well as providing comprehensive information such as particle counting and sizing which the TEM technology cannot match. Establishing a reliable and robust flow cytometry-based set-up specialized for exosome analysis is vital for its ongoing research not only because time and labour saving for obtaining equal amount of information, also allows researchers to enhance their understanding in more complex exosomes-mediated pathways by providing them multi-dimension

data. However, limitations such as heterogeneity, low refractive index and small size make the application of conventional flow cytometry to analysis exosomes become not reliable and accurate. Therefore, we attempted to optimize a flow cytometry-based method to characterize B cell exosomes.

Preliminary experiment was performed where serially ultracentrifuged purified CH12 exosomes were labelled with APC-conjugated IgM and FITC-conjugated IgA and examined by flow cytometry directly. Over 70% of the population expressed neither IgM nor IgA, 23% were IgM positive and less than 4% were IgA positive (Fig. 2A). However, under our flow cytometer configuration, purified exosomes were likely indistinguishable from antibody aggregates based on size or refractive properties (Fig. 2B). In other words, surface Ig profile generated is likely a false positive or false negative result due to the confusion of target population. We therefore need extra analysis to test whether our flow cytometer is capable of resolving particle size differences in the nanoparticle range. To do so, we employed latex beads with known sizes; namely 100 nm, 500 nm and 1 μm as size controls in order to confirm the resolution power of the flow cytometer. However, there was only one population of particles observed based on sizes instead of 3 distinct populations of particles as expected (Fig. 2C). This means our flow cytometer doesn't have enough resolution power to discriminate exosomes and immunofluorescent antibodies aggregates used in this assay based on their sizes.

Since the sizes of nanoparticles weren't a suitable parameter to accurately analyse exosomes using flow cytometry, we attempted to fluorescently label exosomes via staining the parental cells with protein dye (CellTrace Far Red Cell Proliferation Kit) and the stained proteins should be packaged into exosomes that eventually gets released into the exosomal cargo (Fig. 2D). Subsequently, the exosome population

can be distinguished from antibodies aggregates based on the expected differential fluorescence emission rather than size difference. CSR efficiency of CellTrace labelled CH12was validated in order to confirm the core process of the study, B cell CSR, wasn't disturbed by the CellTrace protein dye (Fig. 2E & 2F). Next, exosomes released from CellTrace labelled CH12, with and without stimulation for CSR, were collected after 48 hours, labelled with FITC-IgA and analysed by flow cytometry. CellTrace fluorescent signals from negative controls including PBS, cell culture media and cell culture media with FITC-IgA were used to determine the threshold for positive and negative CellTrace population (Fig. 2G). CellTrace positive population of each sample were gated and the corresponding IgA profile was analysed. However, we could not detect any distinct separation of IgA positive or negative peaks generated from the gated population and we couldn't confidently determine the profile of exosomal surface Ig by this approach (Fig. 2H).

Since the sizes of exosomes are below the detection limit of conventional flow cytometers which means it is unlikely to distinguish exosomes from cytometer background noise (Figure 2I), thus, exosomes have to first bind to larger antibodies coated beads in order to be detected. We coupled anti-IgM antibodies with 3 μm latex beads to produce antibodies coated beads. The beads were then incubated with purified exosomes derived from inactivated and activated CH12 for CSR to form the exosome-bead complexes. The complexes were immunofluorescent stained with anti-IgM and anti-IgA antibodies separately and data was acquired using flow cytometry. A distinct population of particles representing the exosome-bead complexes was identified and distinct from the background noise in the forward and side scatter plot (Figure 2J). The exosome-bead population was gated (Figure 2J) and surface Ig composition of both inactivated and activated CH12 exosomes is shown in (Figure 2K). However, possibly due to the low density of exosomal surface

Ig immunofluorescence to be detected by the cytometer, differences in IgM or IgA positive percentages from both populations were barely noticeable.

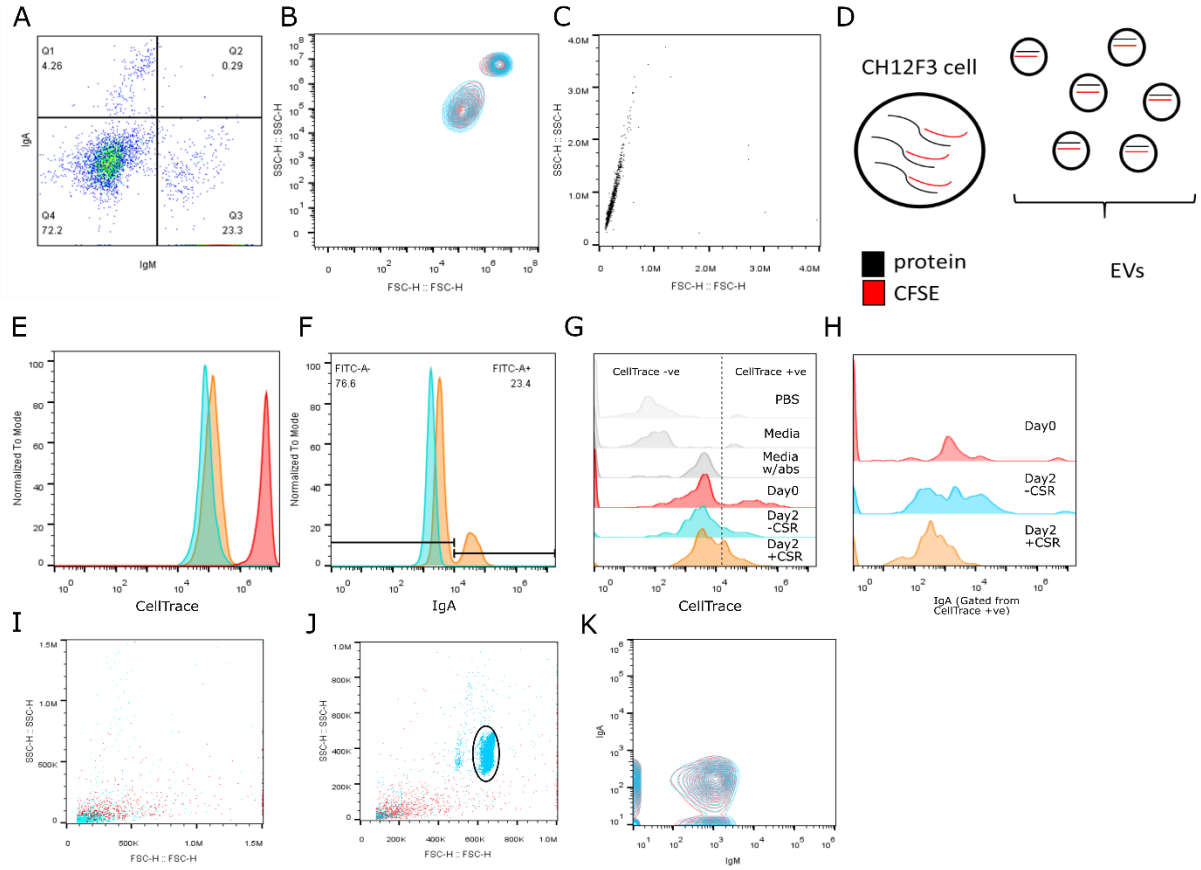

Fig. 2 *CellTrace labelling dependent and antibody coated beads dependent flow cytometry-based analysis of exosomes*. A) Surface IgM/IgA profile of purified CH12 exosomes. B) Cytogram shows forward scatter versus side scatter, purified exosome population in blue and antibodies aggregates in red. C) Cytogram shows forward scatter versus side scatter, combination of different sizes of latex beads. D) Schematic outline of CellTrace labelling dependent exosomes analysis approach. E) Flow cytometry analysis showing the incorporation of CellTrace dye to CH12 cells, Day 0 in red, Day 2 unswitched in blue, Day 2 switched in orange (n=3 per group). F) Flow cytometry analysis of CellTrace labelled CH12 cell CSR from IgM to IgA, ±activation after 48 hours, unswitched in blue, switched in orange (n=3 per group). G) Flow cytometry analysis of CellTrace labelled CH12 exosomes and controls (n=3 per group), line: Threshold for CellTrace positive and negative population. H) Flow cytometry analysis of CH12 exosomal surface IgA from CellTrace positive population. I) Flow cytometry-based detection of exosomes. Blue population represents purified exosomes; Red population originate from filtered PBS only, representing background noise. J) Flow cytometry-based detection of exosomes coupled with antibody-coated beads. Distinctive population of exosome-bead complexes shown in blue was gated and background noise in red. K) Flow cytometry analysis of surface Ig on CH12 exosomes. Blue population represents inactivated CH12 exosomes; Red population represents activated CH12 exosomes.

6.2.1 Validation of GW4869 inhibitory effect on exosome production

Following our efforts to characterise exosomal particles we now shifted our attention to understand the biological functions of exosomes. To validate the inhibitiory effect of exosome production we used a widely used inhibitor known as GW4869. In brieft, GW4869 inhibits the enzymatic function of neutral sphingomyelinase (n-SMase) which hinders ceramide-mediated inward budding of MVBs and the release of exosomes from MVBs. Cell culture medium from GW4869- and mock- treated CH12 was subjected to TEM imaging. Exosomes were still detectable from GW4869 treated CH12 (Fig. 3A), however, with a significant reduction in density compared to mock treated CH12 (Fig. 3B). Since the GW4869 drug is dissolved in DMSO, which has inherent toxicity to cells, the dose used in this assay was previously determined by using the half maximal inhibitory concentration (IC50) (Figure 3C), whether such inhibitory effect of exosome production is dose dependent is yet to be confirmed.

6.2.2 Exogenous and endogenous exosomes regulate CSR in CH12

To gain insight into the role of exosomes in B cell development, specifically CSR, we activated CH12 to undergo CSR using the cytokine cocktail IL-4/TGF-β/CD40-L stimulation with the depletion of exogenous (originating from fetal calf serum, FCS) and endogenous (originating from the CH2 cells) exosomes. To deplete exogenous exosomes, FCS media was subjected to overnight ultracentrifugation (16) and the supernatant was recovered to use in our experimental cell culture media preparation. For the depletion of CH12 exosomes, CH12 was treated with GW4869, inhibitor of n-SMase which is known to block ceramide production, ultimately reducing exosome shedding from cells into the culture media.

Firstly, the depletion of FCS exosomes alone leaded to near 60% decrease in CSR

efficiency compared to control 48 hours after cytokine stimulation (Fig. 3D). This is suggestive that certain FCS exosomal cargo is essential for efficient CSR. Secondly, the depletion of CH12 exosomes alone has no significant effect in CSR efficiency compared to mock treatment (Fig. 3D). It is also suggestive that, with respect to CSR, CH12 exosomes are dispensable when FCS exosomes are present. Interestingly, depleting both FCS and CH12 exosomes by GW4869 lead to less than 40% decrease in CSR efficiency compared to depletion of FCS exosomes with mock treatment (Fig. 3D). It is plausible then that CH12 exosomes are antagonistic to FCS exosomes with respect to CSR, in other words, CH12 exosomes are potentially inhibitory for CSR.

6.2.3 Complementation with endogenous and exogenous exosomes rescue CSR

To validate the role FCS and CH12 exosomes play in CSR regulation, we attempted to rescue the CSR efficiency decrease caused by absence of FCS and CH12 exosomes via complementing purified FCS and CH12 exosomes to our previous experimental conditions. Exosomes from FCS, inactivated CH12 and activated CH12 were collected as stated in the methods section above.

Naïve CH12 were activated to undergo CSR by cytokine stimulation in exosome-free cell culture medium, with mock, GW4869 treatment and no treatment as control. Each condition was complemented with FCS, inactivated CH12, activated CH12 derived exosomes and no exosomes as control respectively. After 48 hours post cytokine stimulation, FCS exosomes complemented conditions including no treatment and GW4869 treatment have recovered CSR efficiency lost up to 92% compared to CSR in FCS exosome-containing cell culture medium which has been

set as 100% (Fig. 3E).

Interestingly, exosomes derived from inactivated and activated CH12 showed contrasting effects on CSR. All inactivated CH12 exosomes complemented conditions exhibited a significant reduction in CSR compared to control which is corresponding to our previous observation. Whilst in activated CH12 exosomes complemented with GW4869 treatment condition, the impaired CSR efficiency was rescued and surpassed the no treatment control, but not the FCS exosome-containing cell culture medium condition (Fig. 3E). This indicates exosomes derived from activated CH12 have opposite effect to exosomes derived from inactivated CH12. In other words, activated CH12 exosomes itself might have a role in positively promoting CSR in other neighbour naïve B cells. Indeed, more work needs to be done in order to reveal the molecular constituents within these exosomes and to understand the interplay between these exosomes and recipient cells in order to establish the underlying mechanism of this observed effect.

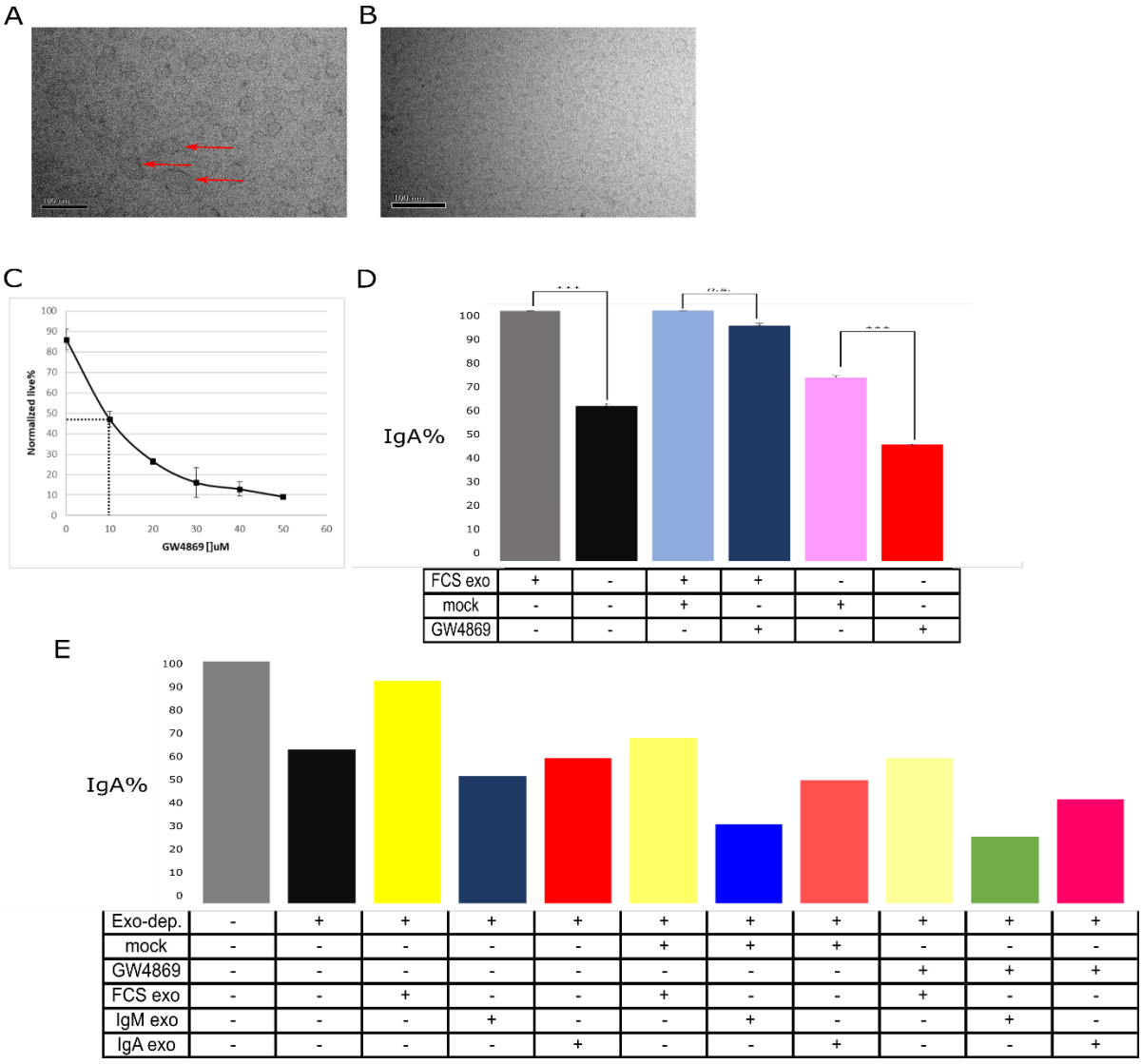

Fig. 3 *CSR efficiency is regulated by exogenous (fetal calf serum FCS-derived) and endogenous exosomes.* A) TEM of isolated exosomes from mock treated CH12. Red arrows indicate presence of exosomes. B) TEM of isolated exosomes from GW4869 treated CH12, no detectable exosomes presented. C) Determination of half maximal inhibitory concentration IC50 of GW4869 by flow cytometry, x-axis: GW4869 concentration, y-axis: % of live cells (n=3 per group). Data shown the mean of the three independent experiments. ± Standard deviation is shown; *p<0.05. D) CH12 CSR from IgM to IgA with the absence of exogenous exosomes (black), absence of endogenous exosomes (dark blue) and absence of both exogenous and endogenous exosomes (red). (n=3 per group), ± Standard deviation is shown; *p<0.05. E) CH12 CSR with complement of FCS-derived (yellow), inactivated CH12-derived (green) and activated CH12-derived (pink) under the depletion of endogenous and exogenous exosomes, presenting data from only 1 independent experiment which has to be repeated for validation.

6.3.1 Characterization of exosomal RNA cargo in CH12 cell line

Apart from surface proteins, a number of studies have shown that cargo within exosomes, especially RNA, play a vital role in intercellular communication via targeted gene regulation. From our previous observations, where exosomes derived from different maturation state in CH12 possess contradictory effects towards CSR,

we attempted to isolate and characterize exosomal RNA from both inactivated and activated CH12, in order to unveil their molecular constituents to gain a better understanding of the underlying mechanism.

We compared a commercial total exosomal RNA kit combining both organic extraction and spin column with glass fibre filter to TRI reagent RNA extraction method to ensure the quality and quantity of RNA were measurable and comparable for downstream experiments. Surprisingly, the RNA quality and quantity from the 2 methods were significantly different. In the commercial kit method, the RNA yield was about 4 ng/μL and the majority of the nucleic acid sized around 150 nt, without the presence of 18s or 28s rRNA (Fig. 4A, 4B). In the TRI reagent method, the RNA yield was around 100ng/μL and the nucleic acids were enriched in multiple size regions ranging from 100 nt to 4000 nt with the presence of 18s and 28s rRNA (Fig. 4A, 4B) which correspond to (3) findings in lymphoblastoid cell lines. This suggested that glass fibre filter column-based kits tend to select for small RNAs whilst TRI reagent method is better in capturing total RNA from exosomes. Based on the yield and the RNA profile compared to published data, we selected TRI reagent-based method to extract exosomal RNA from all of our samples.

6.3.2 Selective packaging of RNA cargo during CSR in exosomes

To understand the molecular constituents contributing to either promotion or inhibition of CSR via exosomal pathway, we extracted RNA from inactivated and activated CH12 and their exosomal RNA. Tapestation analyses that measures cellular RNA quantity and quality suggested that no significant changes in RNA species exist before or after CSR within B cells but the exosomal RNA profile appeared quite different from the parental cells. In cellular RNA, a single clear peak detected at around 100 nt which might represent small non-coding RNAs plus 18s

and 28s rRNA peaks (Fig. 4C). Exosomal RNA species, on the other hand, exhibited multiple clear peaks ranging from 100 nt to 600 nt which possibly represent small non-coding RNAs together with 18s, 28s rRNA peaks and 2 peaks around 1200 nt and 3000 nt which might represent long non-coding RNA (Fig. 4D). During CSR, the amount of each RNA species found in exosomes were significantly transformed. Before CSR, the amount of small non-coding RNA sized from was enriched compared to post CSR; whilst the amount of rRNA and long non-coding RNA post CSR was significantly increased (Fig. 4D). This suggests that CH12 selectively package the exosomal RNA cargo during CSR. Indeed, it is yet to be confirmed whether such exosomal RNA transformation is the cause of CSR promotion via exosomal pathway but it is an interesting prospect given the role ncRNA has been shown to play in CSR efficiency (18) (20).

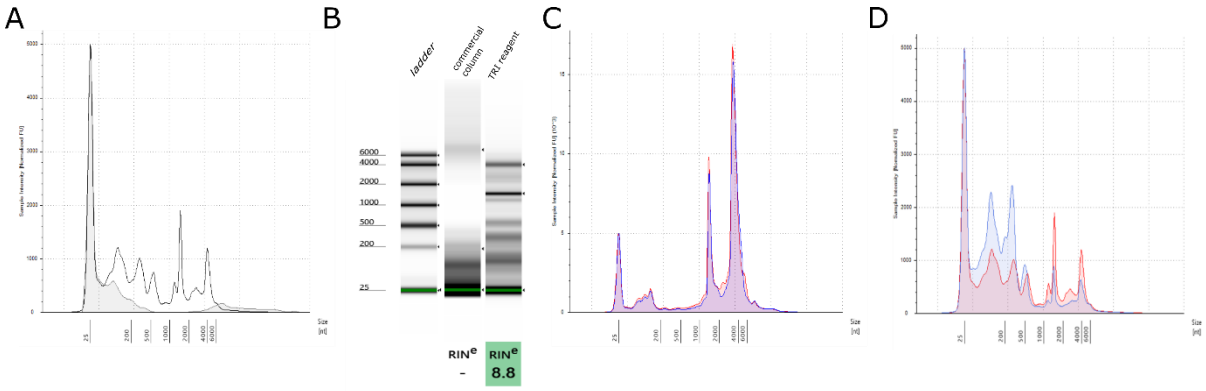

Fig. 4 *Characterization of CH12 exosomal RNA cargo*. A) Electropherogram showing CH12 exosomal RNA isolated with commercial column kits (grey filled) and with TRI reagent (black open). B) Virtual gel image and RIN score corresponding to (A). C) Electropherogram showing CH12 cellular total RNA, ±CSR after 48 hours, blue, -CSR; red, +CSR (n=3 per group). D) Electropherogram showing CH12 exosomal total RNA, ±CSR after 48 hours, blue, -CSR; red, +CSR (n=3 per group).

6.3.3 Testing enrichment of certain ncRNA during CSR activation

To further understand the role of exosome in CSR by the means of enriching and shuttling certain non-coding RNA between B cells, we attempted to quantify the expression variance of CH12 CSR related genes including activation-induced

cytidine deaminase (AID), switch region alpha (Sα), switch region mu (Sμ) and Sμ lariat, in cells and exosomes by RT-qPCR. Briefly, total RNA isolated from CH12 cells and exosomes, ± stimulation for CSR. Isolated RNA was reverse transcribed to cDNA and subjected to qPCR for the expression of the genes listed above relative to β-actin.

From our preliminary qPCR results from cellular RNA, the concentration of Sα in switched CH12 was 20% more compared to unswitched CH12, despite the increase was expected to be around 10 times instead. Interestingly, concentration of Sμ lariat in switched in switched CH12 was double compared to unswitched CH12, indicating Sμ lariat was enriched during CSR in cells. Concentration of both Sμ and AID in switched CH12 were far less than unswitched CH12 which didn't correspond to published data that both genes express at a constant level before and after CSR (Fig 5A).

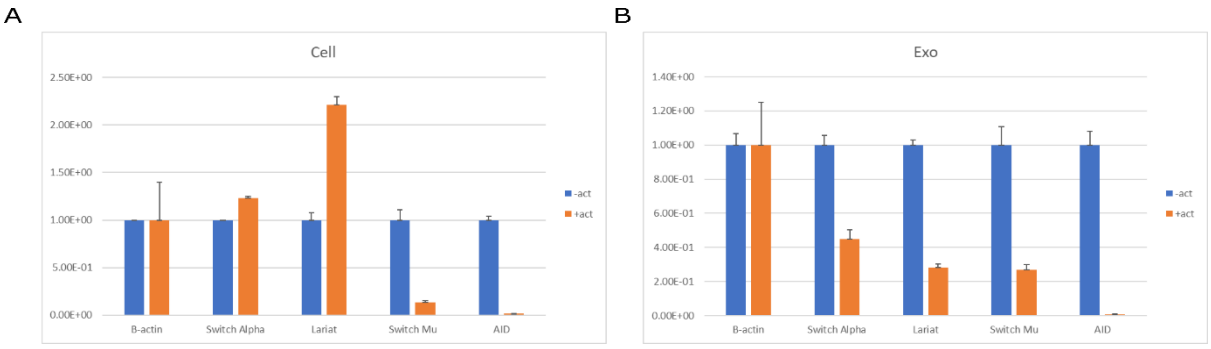

Fig. 5 *Testing enrichment of certain ncRNA during CSR activation by RT-qPCR.* A) Expression of AID, Sα, Sμ and Sμ lariat in CH12 cells, ± stimulation for CSR, normalized to β-actin. Data represents the average of 3 independent experiments. ± SD. B) Expression of AID, Sα, Sμ and Sμ lariat in CH12 exosomes, ± stimulation for CSR, normalized to β-actin. Data represents the average of 3 independent experiments. ± SD.

Whilst from the qPCR results in exosomal RNA, the concentration of all 4 CSR related transcripts from switched CH12 derived exosomes were decreased compared to unswitched CH12 derived exosomes. Concentration of Sα in switched CH12 derived exosomes were around 60% less than that in unswitched CH12 derived exosomes. Concentrations of Sμ lariat and Sμ in switched CH12 derived

exosomes were around 80% less than that in unswitched CH12 derived exosomes. AID concentration in switched CH12 derived exosomes was 1000 times less than that in unswitched CH12 derived exosomes (Fig 5B).

6.3.4 Characterization of exosomal RNA cargo in primary B cells

In addition to studying CH12 cell lines, we also investigated the exosomal RNA cargo in primary B cells for comparison and confirmation. Since cell lines are prone to genetic and phenotypic drift as mutation occurs and results generated could be varied from parental origin to certain extent, primary splenic B cells from wild type C57BL/6 were chosen to eliminate the possibility of cell lines-specific phenotypes in CH12. However, there are several intrinsic limitations of using primary B cells in our experimental design. Unlike CH12 which is immortalized and able to proliferate without cytokine stimulation, primary B cells has to be stimulated by T cell derived cytokines to survive and proliferate *ex vivo*, followed by CSR from IgM to the IgG1 or IgG3, respectively. In contrast to CH12 that are able to grow in unstimulated/unswitched state, primary B cells has to be stimulated by cytokines (i.e. IL-4 and LPS) and undergo CSR in order to survive and proliferate once isolated from the spleen, otherwise more than 99% of the cell population die within overnight after isolation from spleens (21). This created a technical problem for our analysis of primary B cells due to the lack of legitimate unstimulated primary B cells and exosomes derived from them to use as control. Therefore, unlike with CH12, we isolated exosomes from primary B cells every 24 hours in order to thoroughly trace quality and quantity of the exosomal RNA as their parental cells were proliferating and underwent CSR. In addition, on our hands, the amount of exosomal RNA isolated from primary B cells derived exosomes were 10 times less than that in CH12 derived exosomes which made downstream quantitation and qualification even more challenging.

Interestingly, primary B cells were able to grow but remain unswitched for 36 hours after isolation from spleen just by incubating them with exosomes derived from switched CH12 without any cytokine stimulation. The live cell percentage in this condition was about 30% less than that in cytokine stimulated condition (Fig 6A). This phenotype hasn't been reported previously and it suggested that the certain exosomal cargo from switched B cells were aiding cell survival akin to T cell derived cytokines. In addition, the efficiency of primary B cell CSR from IgM to IgG1 was about 25% 72 hours after cytokine stimulation which was corresponding to published data (22). Surprisingly, in our experimental set up, we managed to increase the CSR efficiency of primary B cells up to 65% 72 hours after cytokine stimulation (Fig 6B & 6C). It seemed that the procedure of isolating exosomes from the cell culture every 24 hours and replacing with fresh media could enhance the CSR efficiency in primary B cells. This indicates certain exosomal cargo from stimulated primary B cells were antagonistic to CSR however this needs further confirmations and an in-depth analysis of the potential mechanisms for such possible phenotype.

Primary B cells exosomal RNA were isolated 24 and 72 hours after stimulation for CSR using commercial column-based kit. Since there was a lack of unstimulated primary B cell derived exosomes control as stated previously, the 24 hours timepoint was our earliest control we could use to isolate an adequate amount exosomal RNA for downstream analysis. Therefore, we chose to isolate exosomal RNA at 24 hours to represent the unstimulated control. Indeed, this wasn't the most ideal control and could possibly vary from the real unstimulated control. Isolated exosomal RNA were subjected to Tapestation analysis (Fig 6D) as done previously. Exosomal RNA isolated 24 hours were enriched in the size range of 100 to 150 nt, which might be small ncRNA and such enrichment was absence 72 hours after stimulation.

Interestingly, exosomal RNA sized 750 to 1200 nt were slightly enriched in the 72 hours sample compared to 24 hours sample. This indicated a selective RNA cargo packaging during CSR in primary B cells like CH12. As mentioned before, the commercial column-based kit seemed to select for small RNA rather than total RNA like TRI reagent isolation. Thus, the true landscape of the exosomal RNA profile and enrichment changes in primary B cells is yet to be confirmed. Furthermore, in depth analysis of exosomal RNA, such as RT-qPCR and RNA-seq are needed to be done to reveal the molecular network involved and to explain CSR efficiency enhancement by the means of removing exosomes in cell culture every 24 hours.

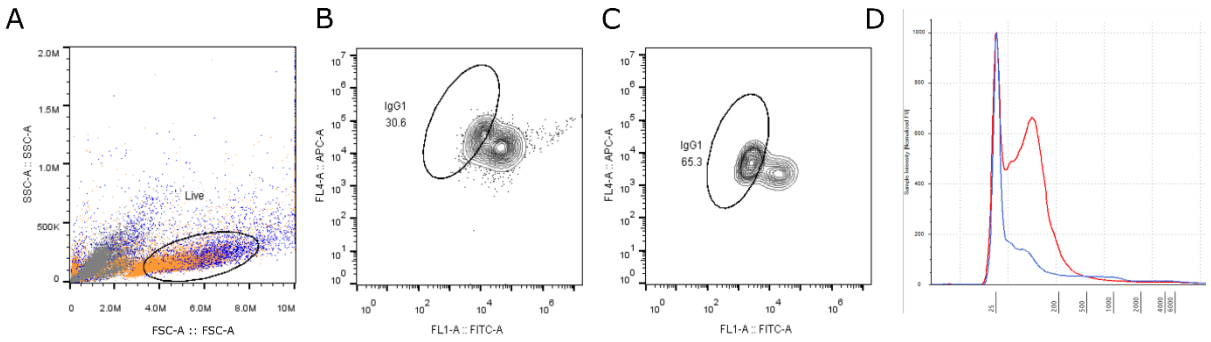

Fig. 6 *Characterization of exosomal RNA cargo in primary B cells.* A) Cytogram showing forward scatter and side scatter, primary B cells without cytokine stimulation in grey, primary B cells incubated with exosomes and without cytokine stimulation in orange and primary B cells with cytokine stimulation in blue, live cell population in oval gate. B) Efficiency of primary B cell (n=3 per group) CSR from IgM to IgG1 (in oval gate), 72 hours after cytokine stimulation without daily exosome removal. C) Efficiency of primary B cell (n=3 per group) CSR from IgM to IgG1 (in oval gate), 72 hours after cytokine stimulation with daily exosome removal. D) Electropherogram showing primary B cell exosomal RNA, 24 hours after stimulation in red and 72 hours after stimulation in blue.

7 Discussion

Emerging evidences revealed exosomes as a novel player in intercellular communication via various mechanisms such as surface peptide interaction and targeted gene regulation. The full potential of exosomes involving in cell to cell communication is yet to be discovered due to their high mobility throughout the human body and remarkably stable structure for preservation and delivery of peptides and nucleic acids between distant cells. Excessive studies have shown exosomes are involved in regulating immune response, especially between T cell and dendritic cells. Apart from direct peptide or antigen presentation, certain pathways are rather complex which involve multi-step and multi intermediate molecules. Understanding the fundamental mechanism would certainly aid to answer various unsolved queries in immunity responses. In this thesis, we attempted to investigate the exosome-mediated B cell to B cell communication pathway through series of experiments, from characterization of B cell exosomes, role of B cell exosomes in CSR to finally looking into the molecular constituents in B cell exosomes derived from different stage of maturation. Regarding to exosome detection approaches, TEM is still the more accurate method to measure the sizes of exosomes as well as surface marker detection using immunogold labelling compared to nanoparticle tracking analysis (23). However, TEM for detecting multiple types of surface marker simultaneously in a clinical application is rather tedious and labor intensives. Also, TEM lacks of the ability of exosomes quantification which is vital for researchers and clinical practitioners in the field to generate quantitative conclusions in experiments. Compared to TEM, flow cytometry-based method is relatively more robust and efficient. Nevertheless, current flow cytometry-based method for analyzing exosomes require experienced users and dedicated flow cytometers to produce reliable results. In order to simplify the complex flow cytometer

customization process and to popularize this method across most available flow cytometers, part of our future work will be optimize the CellTrace-based and immune-beads based flow cytometry method with respect to accuracy and sensitivity. Aside from TEM and flow cytometry, the recent emergence of different types of super-resolution microscopy has been employed in exosome study. Briefly, super-resolution microscopy applied in exosome study is a coupling of conventional optical microscopy and novel optical imaging techniques such as photo-switchable fluorophores in order to overcome the limited resolution of nano-sized particles like exosomes caused by the diffraction limit of light. Super-resolution microscopy also remains the advantages of conventional optical microscopy such as non-invasive imaging and high biochemical specificity. Such breakthrough of resolution limit of optical microscopy has the potential of being an evolutionary tool to study exosomes between TEM and flow cytometry. Firstly, the sample preparation time required for imaging using super-resolution microscopy is significantly less compared to TEM. Secondly, because of the feasibility of colocalization of multiple markers on single exosome particles in super-resolution microscopy, it is possible to gather more comprehensive information about exosome surface molecules compared to TEM (which only allows labelling 1 marker at a time by immune-gold). Furthermore, unlike flow cytometry, optical microscopy-based method is in fact producing images of inputted samples which can eliminate the possibility of false study target in flow cytometry due to improper setup of flow cytometer for studying exosomes. In our study, the reliable labelling and imaging of exosomes offered by super-resolution microscopy hold great potential in the investigation of B cell exosomal surface Ig profile and the interaction between exosomes and parental cells.

Interestingly, in vitro, exogenous exosomes from FCS seemed to be essential for efficient CSR and we are the first to report this information up to our knowledge. As

expected, the underlying mechanism is yet to be established regarding to the intercellular molecular interactions. Additionally, exosomes derived from inactivated CH12 appeared to be inhibiting CSR whilst activated CH12 exosomes showed an enhancing effect in CSR and this experiment has to be repeated to confirm significance of the data. Nonetheless, the exosome inhibition effect by GW4869 treatment is yet to be validated by TEM or flow cytometry in order to confirm the phenotype mentioned above is actually due to depletion of exosomes rather than drug toxicity. Several important information was gathered from the preliminary analysis of exosomal RNA cargo using the Tapestation platform. Different exosomal RNA extraction methods could lead to contrastive conclusions, for instance, commercial column-based kit tended to select for small exosomal RNA and TRI reagent method has a higher coverage of total exosomal RNA. The choice of exosomal RNA extraction approach is certainly vital in order to capture the type of RNA desired for future studies. Also, the difference in exosomal RNA profile between unswitched and switched CH12 clearly indicated a selective exosomal RNA cargo packaging mechanism during CSR. RT-qPCR were then used to test whether certain CSR-related transcripts were involved in such selective exosomal RNA cargo packaging during CSR.

Unfortunately, and possibly due to technical limitations and time constraints at the end of my thesis work, we weren't able to draw confident conclusions. Thus, RT-qPCR with more housekeeping gene controls has to be done in the future in order to validate the expression of CSR-related transcripts and better understand the underlying mechanism of the selective exosomal RNA cargo packaging. Apart from CH12, several optimizations are needed for the validate experiments with primary B cells exosomal RNA. To obtain a legitimate unstimulated/unswitched control, one possible approach is to purify exosomes directly from mouse blood by serial

ultracentrifugation and to capture splenic B cell derived exosomes by magnetic separation using magnetic bead coupled with splenic B cell-specific primary antibodies. Also, TRI reagent method can be applied to extract primary B cell exosomal RNA in order to obtain total RNA for downstream experiments. Later work such as deep sequencing of cellular and exosomal RNA from both inactivated and activated CH12 and primary B cells is essential for us to thoroughly understand the underlying mechanism such as the selective packaging of exosomal RNA during CSR as well as identification of differentially expressed genes which are responsible of the enhancement or suppression in CSR. The succeeding task should be originated from the genes identified in deep sequencing and,by means of gene knockout or overexpression, we hope to gain better knowledge in immune response regulation and immune cells development via exosomal pathway, especially within B cells. Ultimately, through optimizing the whole cascade of experiments we applied in this thesis, we expect to turn this methodology into an alternative platform as a non-invasive diagnostic tool for cancer and autoimmune diseases as well as an exosome-based therapeutic approach.

References

1. *Exosomes: composition, biogenesis and function.* **Clotilde Théry, Laurence Zitvogel & Sebastian Amigorena.** 2, s.l. : Nature Reviews Immunology, 2002, pp. 569-579.
2. *Biogenesis, Secretion, and Intercellular Interactions of Exosomes and Other Extracellular Vesicles.* **Marina Colombo, Graça Raposo and Clotilde Théry.** s.l. : Annual Review of Cell and Developmental Biology, 2014, Vol. 30, pp. 255-289.
3. *Small RNA Sequencing in Cells and Exosomes Identifies eQTLs and 14q32 as a Region of Active Export.* **Emily K. Tsang, Nathan S. Abell , Xin Li, Vanessa Anaya , Konrad J. Karczewski, David A. Knowles, Raymond G. Sierra , Kevin S. Smith and Stephen B. Montgomery.** 1, s.l. : G3, 2017, Vol. 7, pp. 31-39.
4. *Exosomes: Therapy delivery tools and biomarkers of diseases.* **LucioBarilea, GiuseppeVassalli.** s.l. : Pharmacology & Therapeutics, 2017, Vol. 174, pp. 63-78.
5. *Exosomes in bodily fluids are a highly stable resource of disease biomarkers.* **Mathivanan, Stephanie Boukouris and Suresh.** 3-4, s.l. : Proteomics Clinical Applications, 2015, Vol. 9, pp. 358-367.
6. *Cells release subpopulations of exosomes with distinct molecular and biological properties.* **Eduard Willms, Henrik J. Johansson, Imre Mäger, Yi Lee, K. Emelie M. Blomberg, Mariam Sadik, Amr Alaarg, C.I. Edvard Smith, Janne Lehtiö, Samir EL Andaloussi, Matthew J.A. Wood & Pieter Vader.** s.l. : Scientific Reports, 2016, Vol. 6. 22519.
7. *Optimized exosome isolation protocol for cell culture supernatant and human plasma.* **Richard J. Lobb, Melanie Becker, Shu Wen Wen, Christina S. F. Wong, Adrian P. Wiegmans, Antoine Leimgruber, and Andreas Möller.** s.l. : Journal of Extracellular Vesicles, 2015, Vol. 4. 10.3402.
8. *Particle size distribution of exosomes and microvesicles determined by transmission electron microscopy, flow cytometry, nanoparticle tracking analysis, and resistive pulse sensing.* **E. van der Pol, F. A. W. Coumans, A. E. Grootemaat, C. Gardiner, I. L. Sargent. P. Harrison, A. Sturk, T. G. van Leeuwen, R. Nieuwland.** 7, s.l. : Journal of Thrombosis and Haemostasis, 2014, Vol. 12, pp. 1182-1192.
9. *Labeling Extracellular Vesicles for Nanoscale Flow Cytometry.* **Aizea Morales-Kastresana, Bill Telford, Thomas A. Musich, Katherine McKinnon, Cassandra Clayborne, Zach Braig, Ari Rosner, Thorsten Demberg, Dionysios C. Watson, Tatiana S. Karpova, Gordon J. Freeman, Rosemarie H. DeKruyff, George N. Pavlakis, Masaki Tera.** 7, s.l. : Nature Scientific Reports, 2017. 1878.
10. *Role of Lymphocyte Subsets in the Immune Response to Primary B Cell-Derived Exosomes.* **Saunderson SC, McLellan AD.** 7, s.l. : Journal of Immunology, 2017, Vol. 199, pp. 2225-2235.
11. *Exosomal evasion of humoral immunotherapy in aggressive B-cell lymphoma modulated by ATP-binding cassette transporter A3.* **Thiha Aung, Bjoern Chapuy,**

Daniel Vogel, Dirk Wenzel, Martin Oppermann, Marlen Lahmann, Toni Weinhage, Kerstin Menck, Timo Hupfeld, Raphael Koch, Lorenz Trümper, and Gerald G. Wulf. 37, s.l. : Proceedings of the National Academy of Sciences of the United States of America, 2011, Vol. 108, pp. 15336-15341.
12. *Selective extracellular vesicle-mediated export of an overlapping set of microRNAs from multiple cell types.* **Jasenka Guduric-Fuchs, Anna O'Connor, Bailey Camp, Christina L O'Neill, Reinhold J Medina, David A Simpson.** 357, s.l. : BMC Genomics, 2012, Vol. 13.
13. *Mechanism and Regulation of Class Switch Recombination.* **Janet Stavnezer, Jeroen E.J. Guikema, and Carol E. Schrader.** s.l. : Annual Review of Immunology, 2009, Vol. 26, pp. 261-292.
14. *microRNA-155 is a negative regulator of Activation Induced Cytidine deaminase.* **Grace Teng, Paul Hakimpour, Pablo Landgraf, Amanda Rice, Thomas Tuschl, Rafael Casellas and F. Nina Papavasiliou.** 5, 2008, Cell, Vol. 28, pp. 621-629.
15. *Blockade of Exosome Generation with GW4869 Dampens the Sepsis-Induced Inflammation and Cardiac Dysfunction.* **Kobina Essandoh, Liwang Yang, Xiaohong Wang, Wei Huang, Dongze Qin, Jiukuan Hao, Yigang Wang, Basilia Zingarelli, Tianqing Peng and Guo-Chang Fan1,*.** 11, s.l. : Biochimica et Biophysica Acta (BBA) - Molecular Basis of Disease, 2015, Vol. 1852, pp. 2362-2371.
16. *Exosome and Exosomal MicroRNA: Trafficking, Sorting, and Function.* **Jian Zhang, Sha Li, Lu Li, Meng Li, Chongye Guo, Jun Yao, Shuangli Mi.** 1, s.l. : Genomic, Proteomics & Bioinformatics, 2015, Vol. 13, pp. 17-24.
17. *A transcriptional serenAID: the role of noncoding RNAs in class switch recombination.* **Chaudhuri, William T. Yewdell and Jayanta.** 4, s.l. : Oxford Journals International Immunology, 2017, Vol. 29.
18. *Non-coding RNA generated following lariat-debranching mediates targeting of AID to DNA.* **Simin Zheng, Bao Q. Vuong, Bharat Vaidyanathan, Jia-Yu Lin, Feng-Ting Huang, Jayanta Chaudhuri.** 4, s.l. : Cell, 2015, Vol. 161, pp. 762-773.
19. *Induction of exosome release in primary B cells stimulated via CD40 and the IL-4 receptor.* **Saunderson SC1, Schuberth PC, Dunn AC, Miller L, Hock BD, MacKay PA, Koch N, Jack RW, McLellan AD.** 12, s.l. : J Immunol, 2008, Vol. 180, pp. 8146-52.
20. *Noncoding RNA transcription targets AID to divergently transcribed loci in B cells.* **Pefanis E, Wang J, Rothschild G, Lim J, Chao J, Rabadan R, Economides AN, Basu U.** 7522, s.l. : Nature, 2014, Vol. 514, pp. 389-393.
21. *Interleukin-4-mediated Protection of Primary B Cells from Apoptosis through Stat6-dependent Up-regulation of Bcl-xL.* **Wurster AL, Rodgers VL, White MF, Rothstein TL, Grusby MJ.** 30, s.l. : Journal of Biological Chemistry, 2002, Vol. 277, pp. 27169-75.

22. *The ATPase activity of MLH1 is required to orchestrate DNA double-strand breaks and end processing during class switch recombination.* **Richard Chahwan, Johanna M.M. van Oers, Elena Avdievich, Chunfang Zhao, Winfried Edelmann, Matthew D. Scharff, Sergio Roa.** 4, s.l. : Journal of Experimental Medicine, 2012, Vol. 209, pp. 671-8.
23. *Simplified protocol for flow cytometry analysis of fluorescently labeled exosomes and microvesicles using dedicated flow cytometer.* **Vendula Pospichalova, Jan Svoboda, Zankruti Dave, Anna Kotrbova, Karol Kaiser, Dobromila Klemova, Ladislav Ilkovics, Ales Hampl, Igor Crha, Eva Jandakova, Lubos Minar, Vit Weinberger, Vitezslav Bryja.** s.l. : Journal of Extracellular Vesicles, 2015, Vol. 4.
24. *Importance of exosome depletion protocols to eliminate functional and RNA-containing extracellular vesicles from fetal bovine serum.* **Ganesh Vilas Shelke, Cecilia Lässer, Yong Song Gho & Jan Lötvall.** 1, s.l. : Journal of Extracellular Vesicles, 2014, Vol. 3.
25. *Isolation and Characterization of RNA-Containing Exosomes.* **Cecilia Lässer, Maria Eldh, Jan Lötvall.** s.l. : Journal of Visualized Experiments, 2012, Vol. 59.
26. *Modulation of Immune Responses by Exosomes Derived from Antigen-Presenting Cells.* **Ajit, Botros B. Shenoda and Seena K.** 2016, Clinical Medicine Insights: Pathology, Vol. 9, pp. 1-8.